ACIBADEM MEHMET ALI AYDINLAR UNIVERSITY
INSTITUTE OF HEALTH SCIENCES

CELLULAR EFFECTS OF NEUROPEPTIDE Y ON PANCREATIC CANCER CELL MIGRATION TO NEURONS

MENAR EKİZCE
MASTER THESIS

DEPARTMENT OF MEDICAL BIOTECHNOLOGY

SUPERVISOR
Prof. Dr. Güralp Onur Ceyhan

ISTANBUL-2022

ACIBADEM MEHMET ALI AYDINLAR UNIVERSITY
INSTITUTE OF HEALTH SCIENCES

CELLULAR EFFECTS OF NEUROPEPTIDE Y ON PANCREATIC CANCER CELL MIGRATION TO NEURONS

MENAR EKİZCE
MASTER THESIS

DEPARTMENT OF MEDICAL BIOTECHNOLOGY

SUPERVISOR
Prof. Dr. Güralp Onur Ceyhan

ISTANBUL-2022

Department:	Metin girmek için burayı tıklatın.
Program:	Metin girmek için burayı tıklatın.
Thesis Title:	Cellular Effects of Neuropeptide Y on Pancreatic Cancer Cell Migration to Neurons
Student's name and Surname:	Menar Ekizce
Date of Defence:	30/06/2022

This is to certify that I have examined this copy of master thesis. I have found that she/he prepared after fulfilling the specified requirements in the associated legislations before the final examining committee whose signatures are below.

Jury Member (Head of the Defense)	Prof. Dr. Zühtü Tanıl Kocagöz Acıbadem Mehmet Ali Aydınlar University
Jury Member (Thesis Supervisor)	Prof. Dr. Güralp Onur Ceyhan Acıbadem Mehmet Ali Aydınlar University
Jury Member	Assoc. Prof. Hilal Yazıcı Malkoçoğlu TUBİTAK-MAM

DECLARATION

I declare that this thesis work is my own work, I had no unethical behavior at any stages from the planning to the writing of the thesis, I obtained all the information in this thesis in accordance with academic and ethical rules, I cited all the information and comments that were not obtained with this thesis work, and I provided resources in the list of references. I also declare that there was no violation of any patents and copyrights during the study and writing of this thesis.

30.06.2022

Menar Ekizce

PREFACE AND ACKNOWLEDGEMENT

I would like to express my deepest appreciation for my dear advisor Prof. Dr. Güralp Onur Ceyhan and Prof. Dr. Ihsan Ekin Demir for their profound belief and valuable guidance to my work with great experiences. My sincere thanks to you for being the kindest mentors who unwaveringly supported me. I will always be an admirer of your scientific devotement.

The completion of my dissertation would not have been possible without the unparalleled support and nurturing of Dr. Hande Asimgil. I am extremely grateful for all her mentorship as well as friendship throughout the journey. Long lasting earnings will always remind me of her. I am glad to be performed this precious study under her supervision.

I could not have undertaken this journey without my dear lab member Muazzez Gökalp for being just where you need her to be and sharing the hardest periods of this study. I would like to acknowledge the assistance and friendship of Rabia Ünal. I am grateful to these two beautiful, successful lab mates, I had great pleasure of working with them. I also would like to extend my sincere thanks to interns who have contributed to this study.

Lastly, I would like to express my greatest gratitude to my family, cousins and friends for always caring and supporting me through this rough patch. My deepest thanks to my mom Meltem Ekizce and dad Mehmet Ekizce, for their vision, altruism and the invaluable care they showed, for always comforting me about all my doubts and pessimistic thoughts. Also, my brother, Mert Ekizce made me feel at home and cheered me up in every video call, so I thank him for making me such a luckiest big sister. I am deeply indebted to my dearest, precious friend Zeynep Şendil who is always curious about my research, findings and journey. I am and will always be grateful to have these beautiful people in my life.

TABLE OF CONTENTS

LIST OF ABBREVIATIONS AND SYMBOLS

µl	Microliter
µm	Micrometer
°C	Degree Celsius
BCA	Bicinchoninic acid
BSA	Bovine serum albumin
CCK-8	Cell Counting Kit-8
ECM	Extracellular Matrix
ECL	Enhanced Chemiluminescent
EGF	Epidermal Growth Factor
FBS	Fetal Bovine Serum
GEMM	Genetically Engineered Mouse Model
hSC	Human Schwann Cells
HPDE	Human Pancreatic Endothelial Cells
IHC	Immunohistochemistry
mRNA	messenger RNA
nm	Nanometer
NI	Neural Invasion
NP	Normal Pancreas
NPY	Neuropeptide Y
PanIN	Pancreatic intraepithelial neoplasia
PCa	Pancreatic Cancer
PDAC	Pancreatic Ductal Adenocarcinoma
PFA	Paraformaldehyde
PGP9.5	Protein Gene Product 9.5
qRT-PCR	Quantitative Real Time Polymerase Chain Reaction
SDS	Sodium dodecyl sulfate
SFM	Serum Free Medium
TBS	Tris Phosphate Saline
TBST	Tris Phosphate Saline-Tween20
Y1R	Neuropeptide Y 1 Receptor

Y2R	Neuropeptide Y 2 Receptor
Y4R	Neuropeptide Y 4 Receptor
Y5R	Neuropeptide Y 5 Receptor

LIST OF FIGURES

LIST OF TABLES

ÖZET

Nöropeptit Y'nin Pankreas Kanseri Hücrelerinin Sinirlere Migrasyonuna Hücresel Etkileri

Beş yıllık sağkalım oranı %5 olan pankreas kanserinin en yaygın türü Pankreatik Duktal Adenokarsinomdur (PDAC). Son derece agresif olmasıyla da ilişkilendiren PDAC'nin 2030 yılına kadar ikinci önde gelen kansere bağlı ölüm nedeni olması bekleniyor. PDAC'yi bu kadar ölümcül yapan nedenlerden biri, geç teşhis edilme eğilimidir. Teşhis edildiğinde genellikle yakındaki doku ve organlara yayılmış durumdadır. Nöral invazyon (NI), pankreas kanserinde (PCa) sağkalım için bağımsız bir prognostik faktördür ve PDAC'nin ayırt edici özelliği olduğu bilinmektedir. İnvazyon ve metastas, önemli bir araştırma alanı oluşturan sağlam ve karmaşık bir ilişkiye sahiptir. Bu minvalde, tümör-konak mikroekolojisi, hücreler arasındaki karşılıklı etkileşim ve kanser hücrelerinin göçünün altında yatan mekanizmaları içerir. Nöropeptid Y'nin epilepsi, metabolik bozukluklar, nöroblastom ve meme kanseri dahil olmak üzere bazı kanser türleri gibi çeşitli hastalıklarda rol oynadığı bulunmuştur. Ayrıca, pankreas kanserinin nöro-invazif fare modelinde aşırı ifade edildiği tespit edilmiştir. Bu çalışma, pankreas kanseri hücreleri ve nöronlar arasındaki NPY aracılığıyla sağlanan sinyal yolaklarının moleküler ilişkisini ve hücresel etkilerini anlamayı amaçlamıştır.

Anahtar Sözcükler: Pankreas kanseri, pancreatic duktal adenokarsinoma, sinir invazyonu, nöropeptit Y, hedefli migrasyon.

ABSTRACT

Cellular effects of Neuropeptide Y on Pancreatic Cancer Cell Migration to Neurons

The most common type of pancreatic cancer with a percentage of 95 is Pancreatic Ductal Adenocarcinoma (PDAC), associated with a dismal 5-year survival rate of <5%. In relation to being extremely aggressive, PDAC is expected to be the second leading cause of death by 2030. One of the reasons that make PDAC so deadly is its tendency to be diagnosed late. It has already spread to nearby tissues and organs when it is diagnosed. Neural invasion (NI) is an independent prognostic factor for survival in pancreatic cancer (PCa) and is known to be a hallmark of PDAC. Invasion and metastasis have a solid and complex relationship, creating an attractive search field. In this manner, tumor-host microecology contains the crosstalk between cells and underlying mechanisms behind the migration of cancer cells. Neuropeptide Y is involved in various diseases such as epilepsy, metabolic disorders, and cancer types including neuroblastoma and breast cancer. It is also detected as overexpressed in a neuro-invasive mouse model of pancreatic cancer. This study aimed to understand the cellular effects of NPY-mediated crosstalk between pancreatic cancer cells and neurons.

Keywords: Pancreatic cancer, pancreatic ductal adenocarcinoma, neural invasion, neuropeptide Y, targeted migration.

1 INTRODUCTION AND AIM

Pancreatic cancer has a dramatic perception with its extremely high mortality rate and so unlikely early diagnosis. In 2021 cancer statistics, cancer of the pancreas has the lowest survival rate, and it is now the third leading cause of cancer-related death (1). It is seen in the autopsy reports that local tumor recurrence after radical surgery in patients with resectable tumors is very high, with a percentage of 75-80 (2). Despite the improvement in understanding of cancer biology and advancements in cancer therapy, the gap between basic science and clinical approach is challenging to close. Translational medicine, at this point, plays a remarkable role by offering rapid conversion between bench to bedside.

Neural invasion (NI) is a hallmark of pancreatic cancer adenocarcinoma (PDAC) by its occurrence in almost all pancreatic cancer patients (3). Investigating NI was a challenge because of the widely lacking *in vivo* models. My supervisor's group engineered a genetically engineered mouse model (GEMM), TPAC, that develops human-like pancreatic cancer meaning that cancer cells encircle the nerves and show neural invasion. This model enabled pancreatic cancer research to be closely associated with human pathogenesis. Tumor tissue samples from neuro-invasive mouse models were subjected to transcriptome analysis. Neuropeptide Y (NPY) significantly changed when tumor samples from the non-neuro-invasive mouse model were compared. The curiosity about NPY and specifically its cellular effects on cancer cells in terms of increased neural invasion. This study focuses on understanding the potential role of NPY in pancreatic cancer and aims to lead such outputs that could make a major contribution to the translational research of pancreatic cancer. The potential findings of this study and its contributions to future studies may reveal new approaches in the early diagnosis and treatment of pancreatic cancer.

2 BACKGROUND

2.1 Pancreatic Ductal Adenocarcinoma

Pancreas is an endocrine and exocrine organ as such, it takes part in digestion and energy metabolism by producing and secreting both enzymes and hormones. Exocrine pancreas contains highly specialized acinar cells that synthesize, store and secrete digestive enzymes into intralobular and then interlobular ducts which merges to the main pancreatic duct (4). Cancer statistics often use overall 5-year survival to evaluate the prognosis of the disease. Pancreatic cancer is known by its extreme aggressiveness among other gastrointestinal cancers with a dismal 5-year survival rate <5% (5). Pancreatic Ductal Adenocarcinoma (PDAC) is the most common cancer type of the exocrine pancreas with a percentage of 95. It shows a very poor prognosis so that, 24% of patients survive one year after diagnosis (6). In relation to this, pancreatic cancer is expected to be the second leading cause of death by 2030 because of the dramatic increase of the deaths due to this disease (7). This reputation of pancreatic cancer about its mortality is incited by two deficits; lack of effective early detection approaches and effectual therapies. Traditional methods to extend patients survival and relieve the symptoms are chemotherapy, radiotherapy and surgery. Among them, surgery has the most potency for a curative treatment. However approximately 80% of the patients are not eligible for the surgery (8). One of the reasons that makes PDAC so deadly is its tendency to be diagnosed late. Mostly when it is diagnosed, it has already spread to nearby tissues and organs. For the cases at advanced-stages, no certain cure is available (9).

Invasive pancreatic carcinoma classified into two major precursor lesions; pancreatic intraepithelial neoplasia (PanIN) and intraductal papillary mucinous neoplasm (IPMN). Both neoplasms arise in the main pancreatic duct or branching ducts. PanIN is characterized by varying amounts of mucin and degrees of cytologic and architectural atypia and defined as flat or papillary, microscopic, noninvasive epithelial neoplasm. IPMN defined as predominantly papillary, grossly visible, noninvasive mucin-producing epithelial neoplasm. PanIN lesion graded based on the

degree of architectural and cytologic atypia (10). PanIN-1 and PanIN-2 are considered as low grade PanINs, whereas PanIN-3 is considered as high grade PanINs whose progression give rise to invasive PDAC (10). Sequential accumulation of somatic mutations in PanIN lesions are well characterized and documented over time in studies are now known to be driver genes of PDAC. In all grades of PanINs, *KRAS* mutation is the earliest alteration with a rate of 90%. On the other hand, in 70% of high grade PanIN lesions, inactivation of *CDKN2* occurs, while in even later progression of PanIN lesions and invasive PDAC *TP53* and *SMAD4* mutations occurs (11). *KRAS* proto-oncogene is frequently mutated and drives various cancers. Until last years, conventional methods targeting the oncogenic KRAS was not efficient enough, so that gene made name for itself as undruggable KRAS. Growing knowledge about this gene and advances in in molecular technologies emerged novel and more potent therapeutic approaches such as RNAi technology and cancer vaccines (12).

Grading and description of PanIN lesions are based on morphological continuum of dysplastic features and step-wise parallelized accumulation of mentioned genetic alterations (Figure 1). Increasing papillary architecture, cytologic and nuclear atypia, loss of polarity are key features of histomorphological grading of PDAC progression (13).

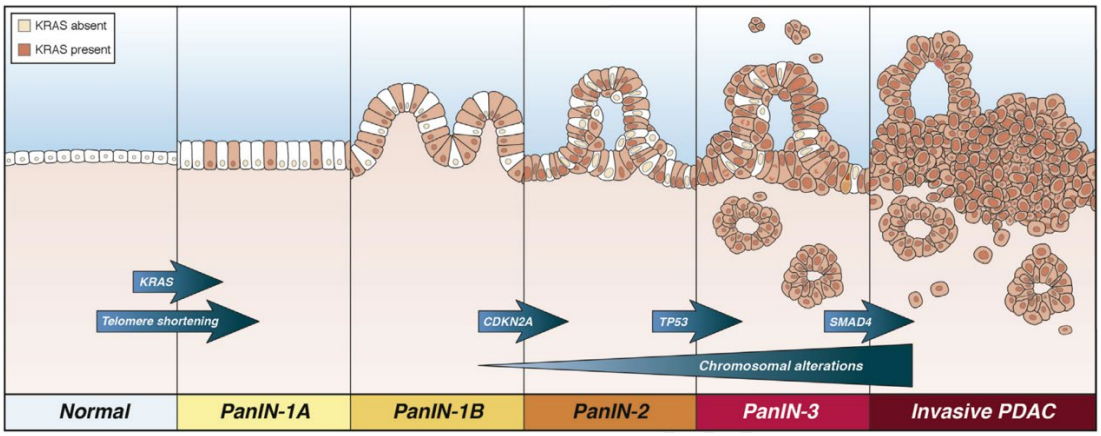

Figure 1. PanIN progression model. Accumulation of genetic alterations in PDAC and illustration of regarding histomorphological features of lesions described by Wood (11).

2.2 Neural Invasion in PDAC

In early 1940's, Neural Invasion (NI) was newly described regarding pancreatic cancer in virtue of observing the carcinoma invading to pancreatic nerves, more specifically endoneural and perineural spaces, and nerves which are in close proximity to pancreas (14). However, nerves have taken attention as a key microenvironmental feature of PDAC in terms of generation and progression of the disease only for the past decade. In PDAC, outstanding plastic alterations of intrapancreatic nerves is seen in the form of neural hypertrophy and increased neural density (Figure 2). NI became a histopathological hallmark of PDAC and an independent prognostic factor for survival and recurrence.

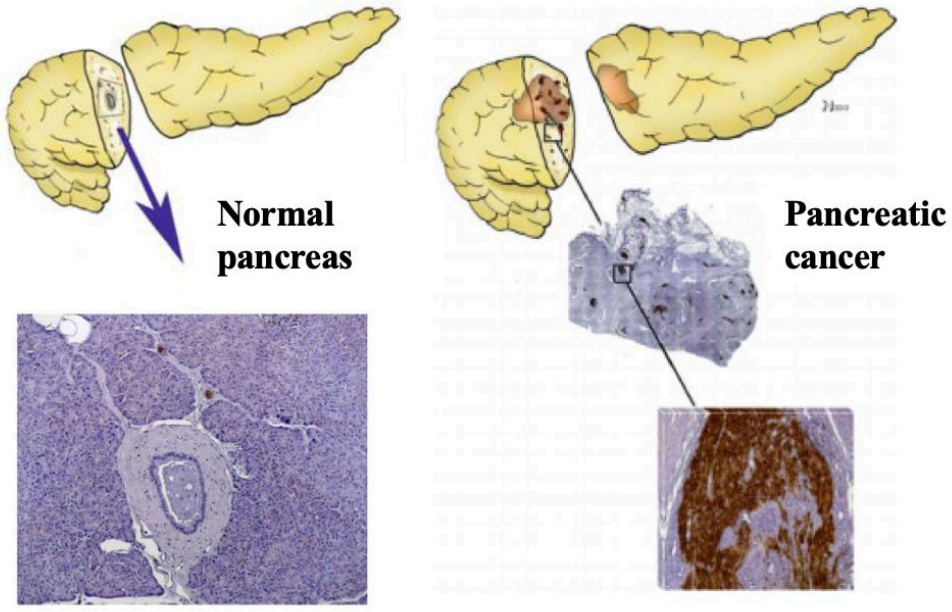

Figure 2. Nerves in the human pancreas and pancreatic cancer. Pancreatic nerves can be visualized by immunolabelling with pan-neural markers like PGP9.5 (brown stained). When compared to normal pancreas, nerves are found to be increased in size and density in pancreatic cancer. Images adapted from Ceyhan (15).

Today, PDAC owns the highest NI severity among all other gastrointestinal malignancies (16). By means of NI, cancer cells use pancreatic neuronal network as a route for metastasis and uncontrollably cause neuropathic pain (Figure 3) which a very dominant symptom in pancreatic cancer patients. Pain is considered as another prognostic factor and present a close relation with NI (17). This intriguing

characteristics of PDAC has given a new perspective to cancer metastasis. It is proposed that, in and around the neuronal spaces more favorable microenvironment is constituted for cancer cells to proliferate and grow along the nerves (18).

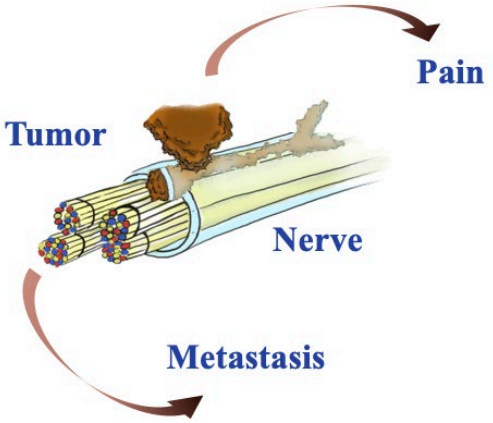

Figure 3. Illustration of neural invasion. Both cancer cells and nerves secrete chemoattractant molecules and modulate the tumor microenvironment which results in migration of cells towards each other and increasing plasticity, eventually cause neuropathic pain and metastasis. Image adapted from Demir (19).

Invasion and metastasis have strong and complex relationship which creates an important field of search. In this manner, tumor-host micro-ecology creates an environment for the crosstalk between tumor, neural and tumor invading immune cells, concomitantly underlying mechanisms behind the migration of cancer cells. Stroma and tumor cells exchange signals so that modifies the local extracellular matrix. These interactions promote proliferation, survival and eventually stimulate migration. Over the years in cancer research, tumor microenvironment gained an enormous importance to elucidate the cancer formation, progression and communication between tumor cells and its neighboring. The nervous system of the organ in which cancer has been originated is considered as one of the neighbors that contribute to the microenvironment (19).

2.3 Genetically Engineered Mouse Models of PDAC

KRAS, *CDKN2A*, *TP53* and *SMAD4* are well characterized driver genes of pancreatic cancer which tends to generate PDAC when they have genetically inherited

or acquired mutations. Gradually accumulation of these mutated genes forms precursor PanIN lesions and eventually give rise to PDAC. Genetically engineered mouse models (GEMMs) are created based on mutations of these driver genes to exhibit the all stages of PDAC similar to its development in humans (20). In human pancreatic tumor neural invasion can be seen in two subtypes: cancer cells encircle nerves which is termed as perineural invasion and penetrate into the interior of nerves which is termed endoneural invasion. One of the most known model is termed "KPC" (*p48*-Cre;LSL-*Kras*^{G12D}; *Trp53*$^{lox/lox}$) which successfully demonstrates the PanIN development. However, this model is not enough to show neural invasion and alterations in neuronal network in pancreas. To address this need, Demir, I. E., proposed a novel mouse model named as "TPAC" (Ptf1a-cre$^{/+}$;Ela-TGFalpha; p53$^{lox/lox}$; p65$^{lox/lox}$) in his PhD thesis, shows human-like neural invasion (Figure 4). TPAC mice is the very first neuro-invasive GEMM of PDAC (3).

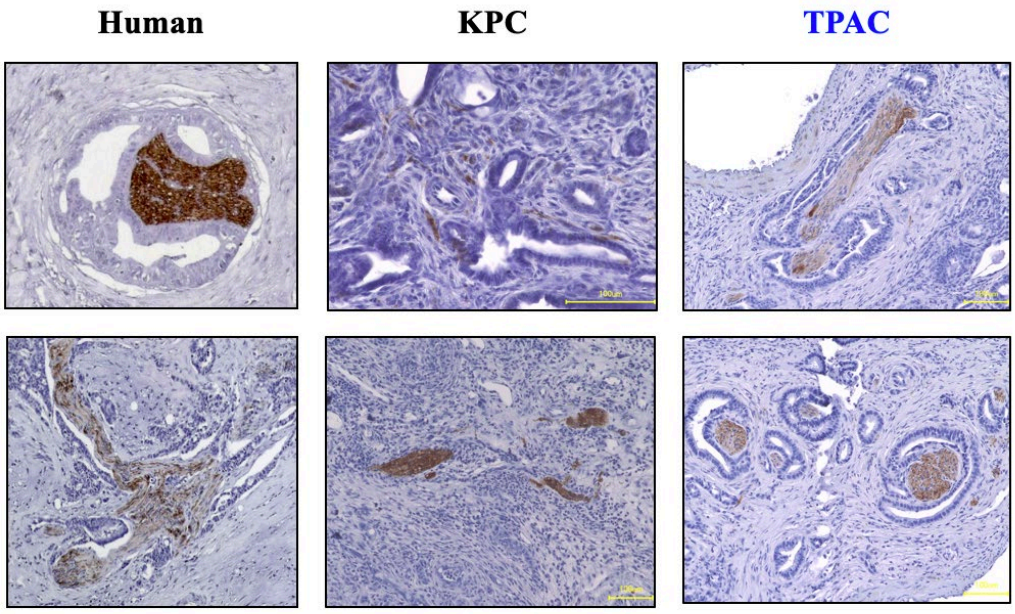

Figure 4. Comparison of neural invasion morphology of pancreatic cancer in human and GEMM of PDAC. Localization of nerves is seen by PGP9.5 immunostaining. In human pancreatic tumor neural invasion is seen in the form of both perineural invasion and endoneural invasion. In KPC model, nerves are occasionally found to be in touch with cancer cells, yet frequently to have not contact at all. In the TPAC model, cancer cells literally encircle nerves around the majority of their borders, corresponding to human-like NI. Images adapted from Ceyhan and Demir. (15, 3).

The investigation of development and mediators in NI has gained importance to understand the nature of this phenomenon and translate the knowledge into clinical cases. Thus, TPAC mouse model has crucial role and impact on this field in terms of in vivo and in silico analyses.

2.4 Neuropeptide Y

Neuropeptide Y (NPY) is a 36 amino acids polypeptide, firstly identified in porcine brain and it belongs to pancreatic peptides family (21). It is a well characterized and expressed neurotransmitter in central and peripheral nervous system. NPY functions via its G-protein coupled receptors called Y1, Y2, Y4 and Y5 in humans (18-22). NPY more widely known as its role in food intake and energy metabolism. Peptide hormones have regulatory effects on neoplasia (23) and it is found to be involved in many and various diseases such as epilepsy, metabolic disorders and cancer types including neuroblastoma, breast, colon and liver cancer (24, 25, 26, 27). Targeting NPY is suggested as a new therapeutic approach for the treatment of prostate cancer in which PNI provides survival for cancer cells (26). Along with the peptide itself, investigational efforts also set sight on expression of NPY receptors in human tumors. In vitro autoradiography showed that Y1 and Y2 receptors (also named as Y1R and Y2R) are expressed in certain carcinomas (28). Function and cellular effects of NPY can differ according to which receptor subtype it is interacting with (29). For instance, hepatocyte-derived NPY interacts with Y5 receptor specifically and promotes hepatocellular carcinoma progression. Moreover, truncated NPY by dipeptidylpeptidase 4 increased Y5 receptor activity and function in liver cancer and terminates Y1R specifity (27). The source of NPY in the tumoral niche can be intratumoral nerves and cancer cells themselves as well which come to mean that NPY signaling may be both paracrine and autocrine (30). Although NPY is a protein that is well studied for a long time, and recently it has compelled attention in cancer studies (22), very less known about its function in pancreatic cancer.

Our group previously generated a large transcriptomic data set from cancer cells isolated from tumors developed in TPAC mice which developed neuro-invasive tumor

(18). When neuro-invasive and non-neuro-invasive mouse models are compared in transcriptomics, NPY was found to be one of the top genes enriched in TPAC cancer cells. The insight that NPY can be an intratumoral mediator of NI gained importance from our point of view.

3 MATERIALS AND METHODS

3.1 Materials

Table 1: List of buffers and components.

Buffer	Components
1x NP-40 lysis buffer	150mM NaCl, 1% NP-40, 50mM pH 8.0 Tris-Cl
1x SDS-PAGE running buffer	25mMTris, 14.41g/l glycine, 1% (v/v) SDS
1x TBS	20 mM Tris, 137 mM NaCl, pH 7.6
1x TBST	20nM Tris, 8g/l NaCl 0.2% (v/v) Tween20, pH 7.6
1x Transfer buffer	25 mM Tris-HCl (pH 7.6), 192 mM glycine, 20% methanol, 0.03% SDS

Table 2: List of consumables, chemicals, solutions and reagents.

Name	Brand	Cat No
NP-40	Thermo Scientific	85124
PhosSTOP EASYpack Phosphatase Inhibitor Tab.	Roche	4906837001
Pierce™ Protease Inhibitor Mini Tablets, EDTA-free	Thermo Scientific	A32955
Pierce ECL Plus WB Substrate	Thermo Scientific	32132
100% Ethanol	Tekkim/isolab	920026
96% Ethanol	Tekkim/isolab	920052
Liquid DAB+ Substrate Chromogen System	Dako	K3468
10% Normal Goat serum	Thermo Scientific	50062Z

Table 2: List of consumables, chemicals, solutions and reagents (continued).

Name	**Brand**	**Cat No**
Citrate buffer 10x-unmasking solution	Vector Laboratories	H3300
Skim Milk Powder	BioShop	SKI400
Restore western blot Stripping buffer	Thermo Scientific	21059
Permanent mounting oil	VectaMount	H-5000
Dako EnVision+ System- HRP Labelled Polymer Anti-Rabbit	Dako	K400311-2
FBS (heat inactivated)	Gibco	10500064
Penicilin/Streptomycin	Gibco	P0781
DBPS	Gibco	14190250
PBS	Gibco	70011044
DMEM High Glucose	Sigma	D5796
RPMI 1640	Lonza	BE12702
Schwann Cell Medium	ScienCell	1701
Keratinocyte SFM	Gibco	17005-034
Keratinocyte-SFM Supplement: Human Recombinant Epidermal Growth Factor (EGF 1-53) & Bovine Pituitary Extract (BPE)	Gibco	37000-015
TrypLE Select	Gibco	12563011
HEPES solution	Sigma-Aldrich	H0887
Trypan Blue solutIon, 0.4%	Thermo Fischer	15250061
DMSO	Sigma	4540
Opti-MEM reduced serum	Gibco	31985070
Lipofectamine RNAimax	Thermo Scientific	13778075
ECM Gel from Engelbreth-Holm-Swarm murine sarcoma	Sigma	E1270
30 %Hydrogen Peroxide	Roth	9681.1
PVDF membrane (0.45 micron size)	Millipore	IPFL85R

Table 2: List of consumables, chemicals, solutions and reagents (continued).

Name	**Brand**	**Cat No**
Adhesion Microscope Slides	Citotest	0303-7191
Microscope Cover Glass	Citotest	0340-3610
Fluorescent Mounting Medium	Dako	S3023
DAPI	Roche	10236176001
16% Paraformaldehyde Aqueous Solution	Electron Microscopy Sciences	15710
Crystal Violet Solution	ChemBio	CB0675
Cell Culture Flask, 75cm^2	Greiner	658970
Cell Culture Multiwell Plate, 6 well	Greiner	657160
Cell Culture Multiwell Plate, 24 well	Greiner	662160
Cell Culture Multiwell Plate, 96 well	Greiner	655180
TC insert, for 24-well plates, PET, translucent, pore size: 8 µm	Sarstedt	83.3932.800

Table 3: List of kits.

Name	**Brand**	**Cat No**
Pierce™ BCA Protein Assay Kit	Thermo Scientific	23227
Cell Counting Kit-8 (CCK-8)	Abbkine	KTA1020
Human NPY ELISA Kit	Merck	EZHNPY-25K
SensiFAST cDNA synthesis kit	Bioline	Bio65054
H&E Staining Kit (Hematoxylin and Eosin)	Abcam	ab245880
SensiFast SYBR No-Rox Kit	Bioline	Bio98005
RNeasy Plus Mini Kit	Qiagene	74134

Table 4: List of antibodies.

Name	Brand	Cat No
Anti-Neuropeptide Y	Abcam	ab10980
Anti-NPY1R	Abcam	ab91262
Anti-NPY2R	MyBioSource	MBS9403698
Anti-beta Actin HRP	Abcam	ab49900

Table 5: List of equipment.

Name	Brand, Cat No
Class II Biological Safety Cabinet	Nuve, MN120
Inverted Microscope Axio Vert.A1	Zeiss, 491237-0007-000
Live Cell Imaging Microscope	Zeiss, Cell Discoverer-7
Incubator	Nuve, EC160
Water Bath	Nuve, NB9
Centrifuge	Thermo Scientific, SL16
Orbital Shaker	Wiseshake, SHO-2D
Microcentrifuge	Beckman Coulter, Microfuge 20R
Pipette	Thermo Scientific
Pipette Filler	Thermo Scientific

3.2 Methods

3.2.1 Cell culturing

3.2.1.1 Culturing human cell lines

Human pancreatic cancer cell lines AsPC-1, BxPC-3, Capan-1, MIA PaCa-2, Panc-1, SU8686, T3M4 were grown in 100mm petri dishes in a 37ºC incubator with 5% CO_2 and passaged once or twice in a week accordingly each line's growing speed. Growth media (RPMI 1640) of AsPC-1, BxPC-3, Capan-1, Panc-1, SU8686, T3M4 cell lines and growth media (DMEM) of MIA PaCa-2 contained 10% FBS and 1% Penicillin/Streptomycin. Human pancreatic epithelial cells HPDE was cultured with

Keratinocyte SFM, supplemented with EGF, bovine pituitary extract and 1% Penicillin/Streptomycin. Mouse pancreatic cancer cell lines KPC, TPC, TPAC and mouse embryonic fibroblast cells NIH3T3 were cultured with DMEM supplemented with 10% FBS, 1% NEAA and 1% Penicillin/Streptomycin. During passaging, cells were washed with 5 ml of PBS after culture media has been aspirated, and then trypsinized with 2 ml of trypsin in 37ºC for 5 minutes and resuspended in appropriate culture media. Cells were centrifuged at 3000 rpm for 5 min. All cell lines were tested for mycoplasma contamination periodically.

3.2.1.2 siRNA transfection

siRNA transfections were performed by using Lipofectamine RNAimax and Opti-MEM reagents. SU8686 cells were seeded in 96-well plates with 2 000 cells/well cell densities in culture media without P/S. For 24-well plates; 20 000 cells/well, for 6-well plates; 200 000 cells/well were seeded. The amount of lipofectamine used for 96-well plate was 1.5 µl lipofectamine and 0.5 µl (5 pmol) siRNA diluted in 25 µl of Opti-MEM as separate tube, for 24-well plates 3 µl lipofectamine and 1 µl (10 pmol) siRNA diluted in 50 µl of Opti-MEM, for 6-well plates 9 µl lipofectamine and 3 µl (30 pmol) siRNA diluted diluted in 150 µl of Opti-MEM. After siRNAs and lipofectamine were mixed with optimem, solutions were mixed well in a 1:1 ratio, incubated at room temperature for 5 minutes. The final siRNA-lipid complex was mixed with the culture media of the cells without P/S dropwise. The final volume of siRNA-lipid complex in Opti-MEM for 96-well, 24-well and 6-well plate formats were 25, 50 and 150 µl respectively. Silencing efficiency of transfected siRNAs listed in Table 6, was measured by Quantitative Real-Time Polymerase Chain Reaction (qRT-PCR). For the functional assays, cells were counted and subjected to interested experiment after overnight incubation of siRNA-lipid complex.

Table 6: List of siRNAs.

Name	Brand	siRNA ID
Silencer Select Pre-designed siRNA, NPY	Thermo Scientific	s9636
Silencer Select Pre-designed siRNA, NPY	Thermo Scientific	s194660
Silencer Select Pre-designed siRNA, NPY	Thermo Scientific	s224125
Silencer Select GAPDH Positive Control siRNA	Thermo Scientific	4390849
Silencer Select Negative Control No.1 siRNA	Thermo Scientific	4390843
Silencer Select Negative Control No.2 siRNA	Thermo Scientific	4390846

3.2.1.3 Cell toxicity assay

Cells were seeded with the previously indicated cell densities in 96-well plates and transfected with siRNA (2.2.1.2). After 2 days, 10 µl of CCK-8 solution was added to each well carefully without introducing bubbles due to O.D. reading interference. Cells were incubated for 1 hour at 37ºC and absorbance were measured at 450 nm using microplate reader.

3.2.2 Molecular biology

3.2.2.3 RNA isolation

Cells were seeded in 100mm plates, after cells were cultured in SFM overnight, collected by cell scraper with ice-cold PBS and centrifuged as indicated in section 2.2.1.1. RNA isolation was done by using Qiagene RNeasy Mini Kit according to manufacturer's instructions. RNA concentration was measured by nanophotometer.

3.2.2.4 cDNA synthesis

SensiFAST cDNA Synthesis Kit was used to synthesize cDNA from isolated RNA bu following manufacturer's instructions. 1 µg of total RNA was mixed with the reaction components according to protocol given in Table 7 and the reaction was performed in thermocycler using the program given in Table 8.

Table 7: Components of reverse transcription reaction.

Reagent	**Concentration/Volume**
Total RNA	1 µg (x µl)
5x TransAmp Buffer	4 µl
Reverse Transcriptase	1 µl
DNase/RNase free-water	Up to 20 µl

Table 8: Thermocycler program for cDNA synthesis

Steps	**Temperature**	**Time (minutes)**
Primer annealing	25 ºC	10
Reverse Transcription	42 ºC	15
Inactivation	85 ºC	5
Hold	4 ºC	∞

After the reaction was completed, all samples were diluted with a 1:10 ratio in DEPC-treated water for the following qRT-PCR experiments.

3.2.2.5 qRT-PCR for mRNA Expression

For qRT-PCR experiments, one reaction mixture per each gene was prepared by mixing the SYBR Green Master mix with the forward and reverse primers of each gene whose sequences are given in Table 9. Volumes of the reaction components were provided in Table 10.

Table 9: List of qRT-PCR primers.

Name	Primer forward (5'-3')	Primer reverse (5'-3')
Human NPY	ATC AAC CTC ATC ACC AGG CAG	CAC CAC ATT GCA GGG TCT TC
Human NPY1R	ATC TGC CCT TGG CCA TGA T	AGG CCA GGT TTC CAG AGA CA
Human NPY2R	GGC TTT CCT CTC GGC CTT C	TGT CAC GGA CAC CTC AGA GTG
Human GAPDH	GTC TCC TCT GAC TTC AAC AGC G	ACC ACC CTG TTG CTG TAG CCA A
Human CYC B	TGT GGT GTT TGG CAA AGT T	GTT TAT CCC GGC TGT CTG TC

Table 10: Amounts of the qRT-PCR reaction components.

Reagent	Volume
SYBR Green	10 µl
Forward Primer (10uM)	0.4 µl
Reverse Primer (10uM)	0.4 µl
Template	4 µl
H_2O	5.2 µl

After distributing 4 µl cDNA per well 96-well PCR plate, 16 µl of reaction mixture was added and carefully mixed by pipetting. The plate was tightly sealed and centrifuged. Plate placed in Bio-Rad CFX96 Touch Real-Time PCR System thermocycler. The reaction was carried out with the parameters shown in Table 11.

Table 11: qRT-PCR program.

Step	Temperature	Duration
1)	95 ºC	3 min
2)	95 ºC	10 sec
3)	58 ºC	30 sec
	+ plate read	
5)	Go to step 2	39 more times
6)	Melt Curve 65ºC to 95 ºC, increment 0.5 ºC	
	+ plate read	
7)	END	

3.2.2.6 qRT-PCR data analysis

Analysis of the qRT-PCR was done by ΔΔCt method using two housekeeping genes; GAPDH and Cyclophilin B. Statistical significance between two groups was tested using Student's two- tailed t-test. Three technical replicates were done for each condition.

3.2.3 Protein biochemistry

3.2.3.1 Protein isolation

Cells were seeded in 100mm plates after cells were cultured in SFM overnight, collected by cell scraper with ice-cold PBS and centrifuged as indicated (section 2.2.1.1.). For the isolation of proteins from whole cell, pellets were lysed completely by mixing with NP-40 buffer. For complete lysis, they were incubated on ice for 20 minutes and agitated vigorously at every 10 minutes. Then, the mixture was centrifuged at 14,000 g for 20 minutes at 4ºC, and the supernatant containing the proteins was collected in a fresh tube. Proteins were kept at -2ºC for further experiments.

3.2.3.2 Protein quantification

Protein quantification was done by using the BCA Assay Kit according to manufacturer's instructions. BSA standard solutions were prepared at 9 different concentration ranging from 0 to 2 µg/µl, and 20µl from each standard was placed in 96-well plate in duplicates mixed with 5µl lysis buffer. 25 µl from each sample previosly diluted 1:5 was also placed in triplicates, and the dilution factor was taken as 5 for subsequent analysis. Working BCA solution was prepared by mixing reagents A and B in a 50:1 ratio and 200 µl of the working solution was distributed. After 30 minutes of incubation at 37ºC, absorbance was measured with the microplate reader at 562nm. Using the absorbance values obtained from BSA standards, a calibration curve was drawn, and sample concentrations were quantified by using the standard curve equation.

3.2.3.3 Sodium dodecyl sulfate polyacrylamide gel electrophoresis (SDS-PAGE)

Concentrations of protein samples were equalized by mixing appropriate amounts of protein solution with water and 6X protein loading dye. Immediately after mixing with the loading dye, the samples were boiled at 95ºC for 5 minutes. Polyacrylamide stacking and resolving gels were prepared by using the ingredients listed in Table 12.

Table 12: Components of the stacking and resolving gels at different concentrations.

Solutions for preparing 4% stacking gel

Solution components	Volumes for 2 gels (µl)
H_2O	3075
30% acrylamide mix	670
1 M Tris (pH 6.8)	1250
10% SDS	50
10% Ammonium persulfate	25
TEMED	5

Table 12: Components of the stacking and resolving gels at different concentrations (continued).

Solutions for preparing 12% resolving gel

Solution components	Volumes for 2 gels (µl)
H_2O	3200
30% acrylamide mix	4000
1.5 M Tris (pH 8.8)	2600
10% SDS	100
10% Ammonium persulfate	100
TEMED	10

Resolving gel was prepared first, and poured between the thin and 1.0 mm thick glasses. The top of the gel was covered with isopropanol until it was fully polymerized. After polymerization, isopropanol was removed. Stacking gel was casted on top of the resolving gel, and comb was placed inside the stacking gel. 7 µl protein ladder was loaded to the first well and the other wells were filled with samples. Electrophoresis was performed at 90V until samples reach resolving gel, then 120V for 60 min.

3.2.3.4 Western blotting

For semi-dry transfer, sponges moistened in transfer buffer. 0.40 µm PVDF membrane was first placed in 100% methanol for 30 second and then placed in transfer buffer I. The transfer layers were made by putting in the order of 1 transfer sponge, membrane, the gel and 1 more transfer sponge. The stacked layers were placed in Semi-dry Turbo Blot machine and transfer was done for 30 minutes at 25V.

After transfer, PVDF membrane was stained with Ponceu S solution for 5 minutes in order to check if the transfer occurred properly or not. The membrane was washed with ddH2O until Ponceu S stain was completely removed. Then, membrane was cut according to the kDa of the protein of interest and placed in 5% (w/v) milk in TBST blocking solution for 1 hour at room temperature with slow agitation. After removal of the blocking solution, membrane was incubated with the primary antibody solution

overnight at 4ºC or 1 hour at room temperature for loading control protein. List of primary and secondary antibodies were given in Table 4.

After the primary antibody incubation, membranes were washed with TBST for 10 minutes, three times on shaker. Membranes were then incubated in secondary antibody solution for 2 hours at room temperature with slow agitation. After secondary antibody incubation, membranes were again washed with TBST for 10 minutes, three times on shaker. ECL reagents A and B were mixed in 1:40 ratio and applied onto the membranes which were then placed on ChemiDoc. Exposure time differs ranging from 5 minutes to 40 minutes.

3.2.3.5 ELISA

Cells culture supernatants were collected and used as samples for ELISA kits. Manufacturer's instructions were directly followed.

3.2.4 Immunohistochemistry

2,5 μm sections were prepared from paraffin-embedded human and mouse pancreas tissues. After deparaffinization in Roticlear for 10 minutes 3 times, slides were rehydrated in ethanol series in decreasing concentration order starting from 100%, 96%, 70 and 50% for 5 minutes for 3 times, sections then washed in distilled water for 5 minutes 2 times. For antigen retrieval step slides were boiled with citrate buffer at 600W until boiling, afterwards at 90W for 10 minutes and cooled for 20 minutes at room temperature. blocked with normal goat serum to exclude the non-specific binding for 1 hour at room temperature. Then, the sections were incubated with the primary antibody at 4°C overnight. Following a 5 minutes washing with TBST, tissues were encircled with DAKO pen and incubated with 0.5% Triton X100 in PBS for 5 minutes at room temperature for permeabilization step. After one more washing step slides were incubated with 3%H_2O_2 for 5 min to block endogenous hydrogen peroxidase activity. Slides were washed again with TBST prior to blocking step with 10% Normal Goat Serum for 1 hour at room temperature. Primary antibody

incubation was done overnight at 4ºC on shaker. After incubation, the sections were washed with TBST for 10 minutes, 3 times and incubated with Dako Envision+ system-HRP secondary antibody for 1 hour at room temperature. Then, Dako Liquid DAB+ Substrate Chromogen System was used for the color reaction. For counter staining, slides were dipped into hematoxylin and washed under tap water for 15 min. Then they are dehydrated with the same alcohol series and Roticlear in opposite order of concentrations. Finally, slides were subjected to permeable mounting media. Quantification of DAB positive cells in the tissue was done via QuPath.

3.2.5 In vitro functional assays

3.2.5.1 Colony formation assay

SU.86.86 cells were transfected siRNA against NPY and T3M4 cells were treated with 10^{-7}M human NPY for overnight. Then cells were seeded in 6-well plate with 500 cell/well density. Colony growth is monitored daily and experiment is terminated at the day of 13. Culture medium was decanted and wells are washed with PBS. Then cells were fixed with 10% PFA for 5 min and washed with PBS. Cells were stained with crystal violet for 30 min, dye were decanted and plates were gently washed with PBS several times until no dye residues remain. Images of stained colonies on 6 well plate were analyzed with via Image J.

3.2.5.2 Scratch assay

Cells were seeded in 6-well plate with $2x10^5$, 3 $x10^5$and 3 $x10^5$cell/well density for SU86886, T3M4 and HPDE respectively. siRNA transfection and human NPY treatment is applied when cells were 70-80% confluent. After overnight incubation of both treatments, culture medium is decanted, wound was generated using 1000 µl pipette tip and plates were washed with PBS. 2 mL fresh medium were added to the wells and wound healing is observed in live cell imaging microscope Zeiss Cell Discoverer 7 for one day. Images were taken from 3 equal areas from each wound with 6 hours intervals. Analysis is done via ImageJ, measuring wound area. % wound

healing is calculated and statistical analysis was done via GraphPad using one-way ANNOVA. Experiment is replicated 3 times.

3.2.5.3 Trans-well invasion assay

Human Schwann cells were seeded into 24-well plates with 4 x10^5 cells/well cell density. Next day, when they were 80-90% confluent, SU8686, T3M4 and HPDE cells were seeded into inserts with 5 x10^3 cells/insert cell density. Prior to seeding, inserts were coated with 10% ECM containing culture medium for 2 hours in 37 ºC in order to fill the membrane pores with ECM. This will enable experiment to indicate cell invasion toward hSC by moving through ECM. Culture medium of each cells were mixed with hSC medium at 1:1 ratio for the co-culture. After 3 days of incubation inserts were washed with PBS twice, Then, non-invaded cells which are located inside of the insert, in other words, on the top of the membrane were cleaned with PBS soaked cotton swab. Invaded cells at the bottom of the insert membrane were fixed with 4% PFA for 20 min and washed with PBS twice. Cells were stained with 0,25 µg/mL DAPI for 15 min and washed with PBS. Finally, membranes were cut using a scalpel and placed onto microscope slides as invaded cells (bottom of the membrane) facing upwards and slides were covered with fluorescent mounting medium and cover slips. Membranes were scanned and cells were counted via Image J. Invasion index of cells was calculated by the ratio of invaded cells of hSC co-cultures to invaded cells in mono-cultures of the subjected cells. Statistical analysis was done via GraphPad using one-way ANNOVA. Experiment is replicated 3 times.

4 RESULTS

4.1 Immunohistochemical Analysis of NPY in Human Pancreatic Tissue

In order to find out NPY expression in human pancreatic cancer, paraffin sectioned slides of human PCa and normal pancreas were immuno-stained with NPY. A recent study about the expression pattern of NPY in the Gastro-Entero-Pancreatic system showed that NPY immunoreactive cells increased in pancreatic islets (31). Immunostainings showed that NPY is found in both normal pancreatic and pancreatic cancer tissue; some of the nerves, significantly cancer cells, and comparably islets were stained against NPY. Interestingly, when NP and PCa were compared, NPY was predominantly expressed in PCa. Strong positive immunoreactivity was seen in the cell cytoplasm of ductal epithelial cells forming PanIN lesions and tumor cells. Some adjacent stroma was also positively stained. In normal pancreas, while only islets and some nerves were stained, in pancreatic cancer tissues, neoplastic regions, PanIN lesions, and PDAC, certain nerves were intensely stained. (Figure 5).

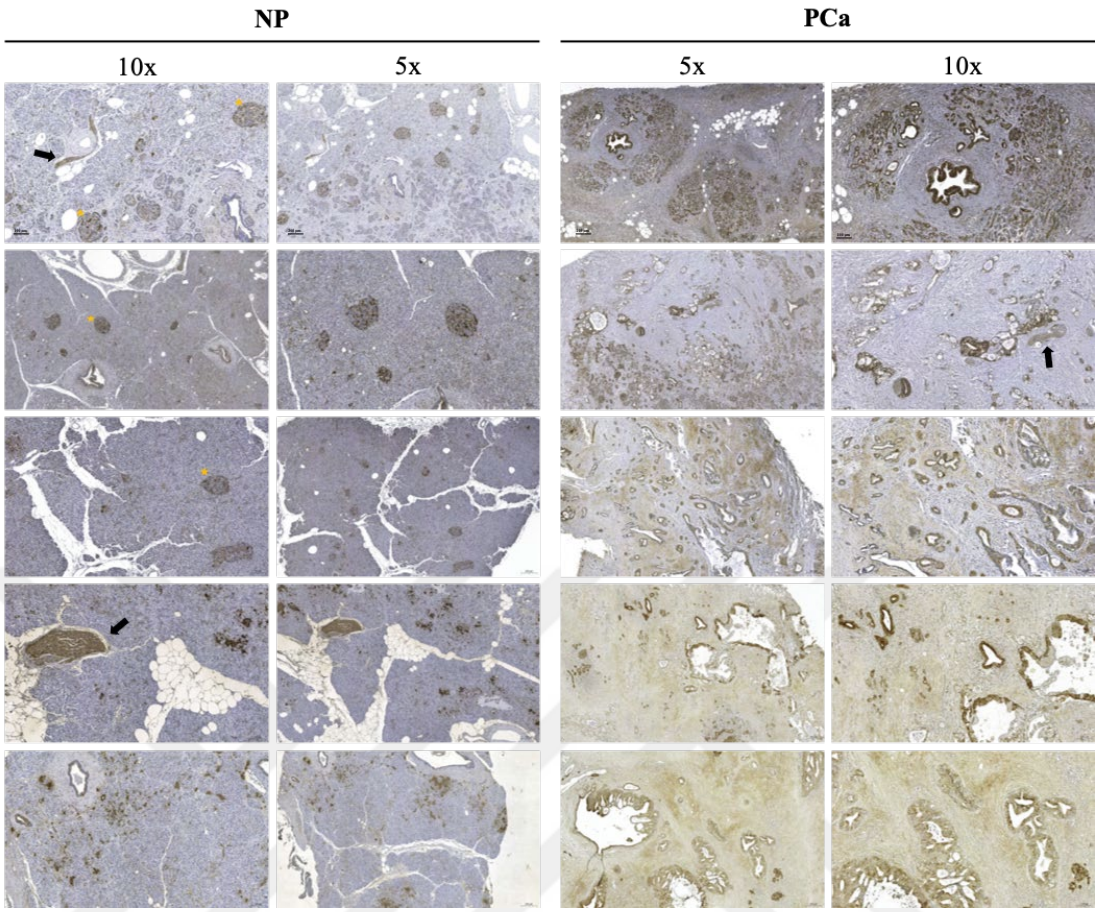

Figure 5. IHC panel for NPY detection in human pancreas. Representative photomicrographs of anti-NPY staining in pancreatic cancer tissue (n=5) and normal pancreas (n=5). Visual examination of DAB positive areas showed that NPY is expressed in pancreatic islets (yellow asterisk) and some of the nerves (black arrow) in both tissues. Differential expression of NPY was observed and significant overexpression was seen in PCa tissue compared to NP.

The results obtained from IHC staining were further analyzed via QuPath to demonstrate the strong positive immunoreactivity of NPY in PCa tissue compared to NP. 5 samples from each group, pancreatic cancer tissue and normal pancreas, were quantified by positive cell count and calculation of the ratio over whole tissue area. Average tissue immunoreactivity against NPY in PCa was 24.6%, while this percentage was found at 5.7 in NP, resulting in NPY being expressed more than four times in cancer tissue compared to normal pancreas tissue. This result showed that expression in cancer tissue significantly increased when compared to NP (Figure 6).

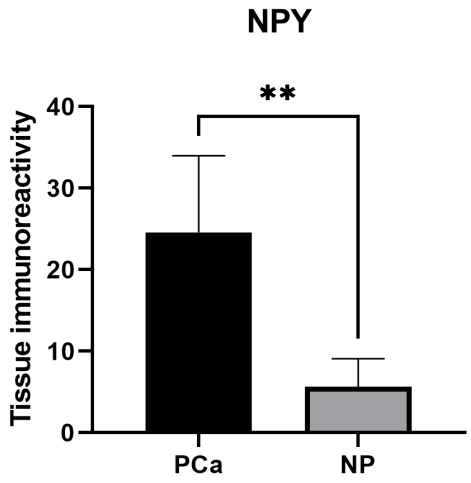

Figure 6. Quantification of differential expression of NPY in PCa and NP tissue. The expression of NPY in human pancreatic cancer significantly increased compared to normal pancreas. Tissue immuno reactivity was measured by DAB-positive cell count via QuPath. Student t-test was applied, ***P=0,0029*.

4.2 Expression Analysis of Human PCa Cell Lines

Augmented NPY expression in human pancreatic cancer tissue led the study to investigate the expression of NPY and its receptor family, NPY1R, NPY2R, NPY4R and NPY5R, in human pancreatic cell lines. Several methods were used for examination at RNA and protein levels. qRT-PCR was used to detect and quantify NPY and receptor family mRNA in cells. ELISA was used to detect secreted NPY in the cell culture supernatant, and immunoblotting was performed to detect receptors in whole protein lysate of cells. The purpose of using multiple PCa cell lines is to determine the highest and lowest NPY expressing cells, then further investigate them to elucidate the effect of expressional modification and complementation of NPY *in vitro.*

4.2.1 Expression profiling of NPY and NPY receptors in human PCa cell lines at mRNA level

Studies up to the present have already shown that NPY is expressed in human pancreatic beta cells (32). In this study, human pancreatic epithelial and human pancreatic cancer cells were examined, and NPY expression profiling was obtained.

qRT-PCR was performed to differentiate basal NPY and its receptors' expression at the RNA level. 5 of the cell lines were found to express NPY at nearly the same level as HPDE. Notably, SU.86.86 was found to have the highest, and T3M4 was found to have the lowest NPY mRNA expression among 7 human PCa cell lines (Figure 7). Both cell lines were derived from metastatic sites and are known to have the unique characteristic of cancer cells as invasive (33, 34). This result is intriguing because these two lines took part at the opposite poles of the cluster while sharing the common invasiveness feature.

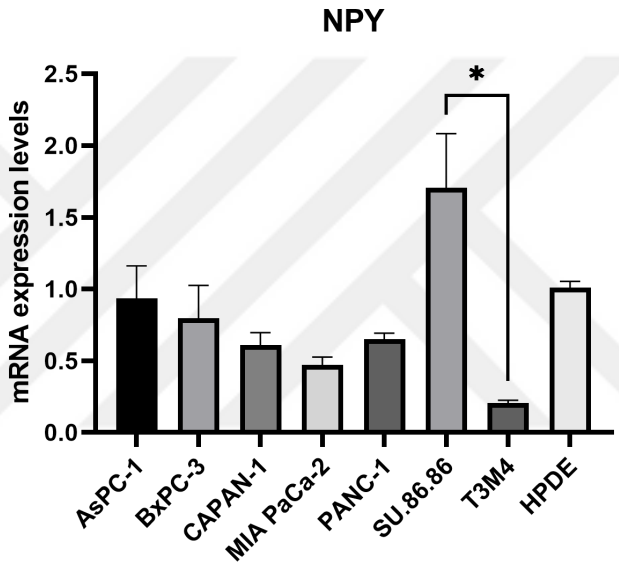

Figure 7. hNPY expression determined by qRT-PCR using hNPY specific primers in human cell lines. mRNA expression levels were calculated using ΔΔCt relative to HPDE and GAPDH was used as the housekeeping gene. n=3, ***P=0.0030*

At mRNA level, NPY receptor type 1 (Y1R) and type 2 (Y2R) from the receptor family were analyzed via qRT-PCR using primers specific to each receptor (Figure 8). Both receptors were expressed in different PCa cell lines. It was seen that Y1R was expressed mainly in SU.86.86 cells. However, none of the PCa cell lines expressed more than HPDE. At RNA level, Y1R was found to have decreased and heterogeneously distributed expression in PCa cell lines compared to ductal epithelial cells, HPDE. In the case of Y2R, except CAPAN-1, PCa cells expressed less Y2R than HPDE. CAPAN-1 was found to have the highest Y2R expression among all PCa cell limes and HPDE at mRNA level.

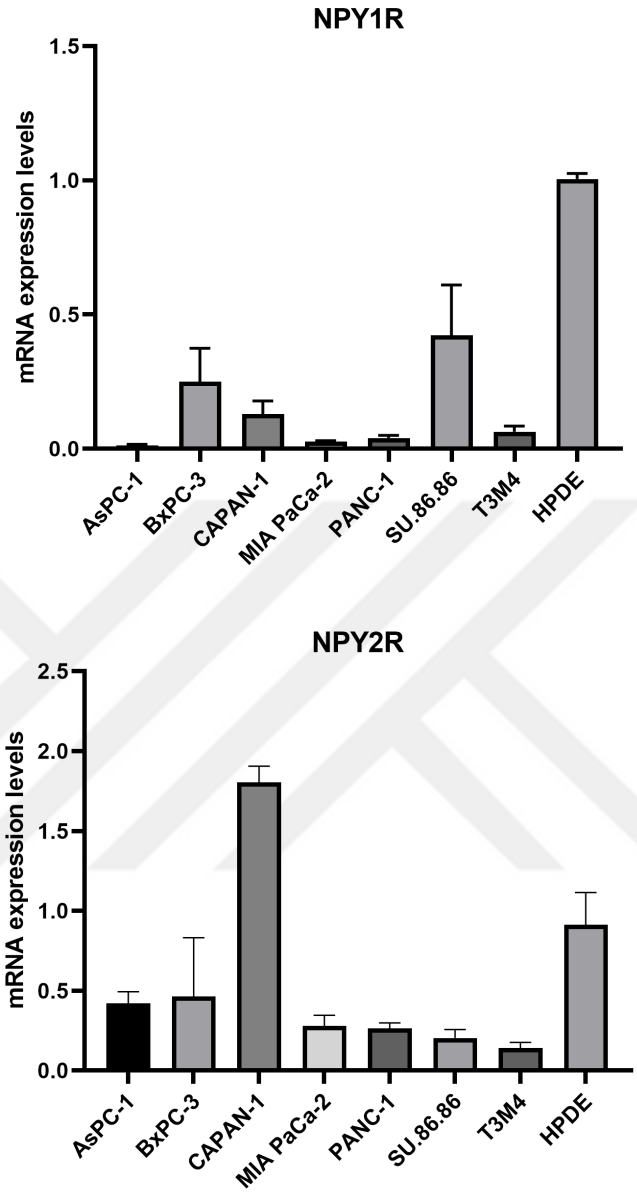

Figure 8. Y1R and Y2R expressions of human PCa cell lines. mRNA expression levels are determined by qRT-PCR analysis and hGAPDH was used as housekeeping gene. ΔΔCt levels were calculated relative to HPDE. n=3, ****p>0.0001.

4.2.2 Expression profiling of NPY and NPY receptors in human PCa cell lines at protein level

At protein level, culture medium of cell lines was collected, and extracellular NPY level was determined by ELISA. Unlike the mRNA expression profile, there was a completely different scenario at secreted protein level. AsPC-1 was found to have the

highest secreted NPY expression among others (Figure 9). BxPC-3 and CAPAN-1 were found to have slightly more NPY expression than HPDE. In general, except AsPC-1, there was no significant difference between the cells in terms of secreted NPY. Human Schwann cells and LN-229 glioblastoma cells also showed similar expression and were not significantly different from HPDE.

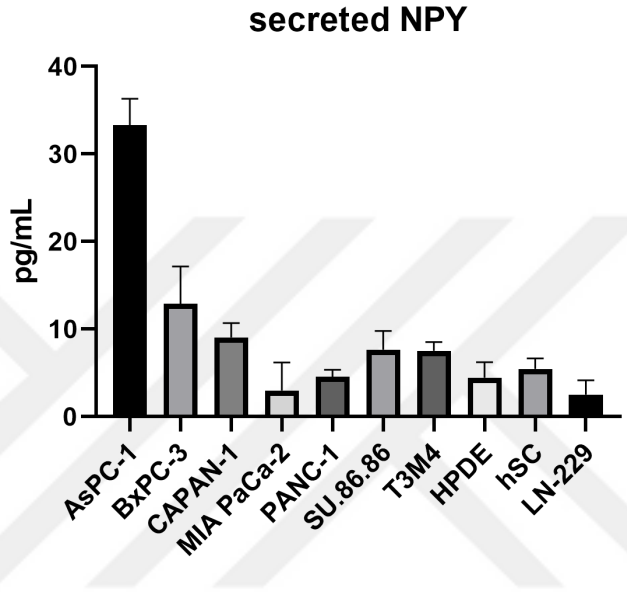

Figure 9. ELISA analysis of NPY production by 10 cell lines. Cell culture supernatant was harvested and subjected to ELISA analysis for NPY detection. n=3, ****p<0.001.

In order to investigate the expression profiles of NPY receptor family in human PCa cell lines at protein level, immunoblotting was performed for each receptor type, Y1R, Y2R, Y4R and Y5R (Figure 10). Unlike mRNA expression, AsPC-1 and CAPAN-1 were significantly overexpressing Y1R. Any signal was not detected in other 5 PCa cell lines and HPDE. For Y2R CAPAN-1 was found to be the most expressing cell line at both mRNA and protein levels. AsPC-1 was also found to be express Y2R; it was the second most expressing cell line at mRNA level. Interestingly, while CAPAN-1 was found to express all receptor types at protein level, other cell lines seemed to be grouped in a way that expressed either Y1R, Y2R or Y4R, Y5R.

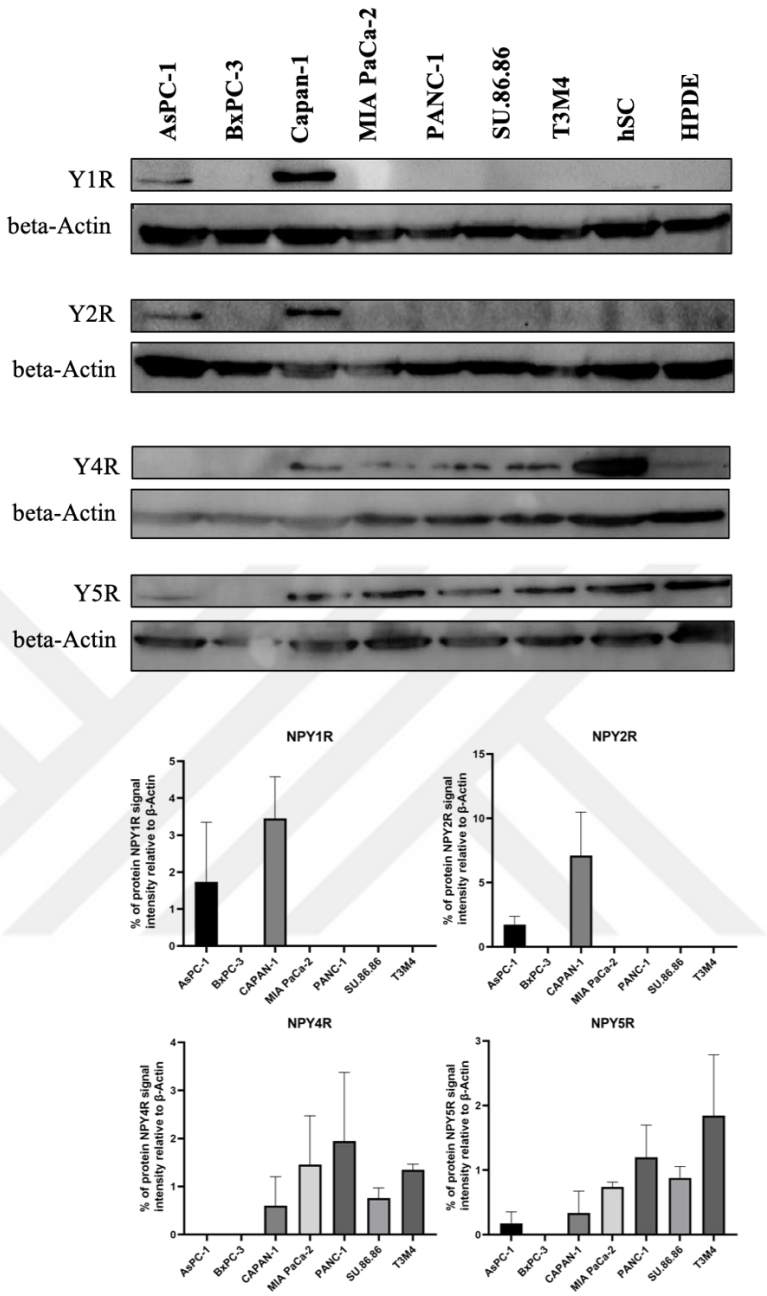

Figure 10. Western blot detection of human NPY receptor subtypes Y1R, Y2R, Y4R, Y5R. 30 µg total cellular proteins were immunoblotted. AsPC-1 and CAPAN-1 expressed Y1R (44 kDa) and Y2R (43 kDa) among 7 PCa cell lines, n=3, ****P=0.0002, ****P<0.001,* respectively. NPY4R (33 kDa) expressed in 5 PCa cell lines among 7 and NPY5R (51 kDa) expressed in 6 PCa cell lines among 7, n=2. Expression profiles of the receptors at protein level can be interpreted as Y1R, Y2R had similar distribution while Y4R and Y5R had the same similarity in the remaining cell lines. Beta-Actin was used as loading control.

4.3 NPY Silencing with siRNA Transfection

Gene manipulation through small interfering RNA (siRNA) was applied to SU.86.86 cells to obtain rapid and cost-effective silencing at the transcriptome level. The subjected cell line was chosen due to expressing the most NPY at mRNA level. Its invasive character made SU.86.86 cells a good choice to further analyze its migratory behavior toward nerves. Cells were transfected with siRNA for NPY depletion. Individual 3 siRNAs targeting NPY were transfected as a mixture. GAPDH siRNA was as a positive control for transfection method, and the mixture of two non-targeting siRNA controls were used as the negative control. Silencing validation was obtained by qRT-PCR analysis (Figure 11). Gene knockdown of hNPY was successfully achieved in SU.86.86 cells by 80% at 20 pmole 2 days after transfection. This result enabled the method to be used for gene manipulation via RNAi silencing in further functional assays, colony formation, scratch, and trans-well invasion assay.

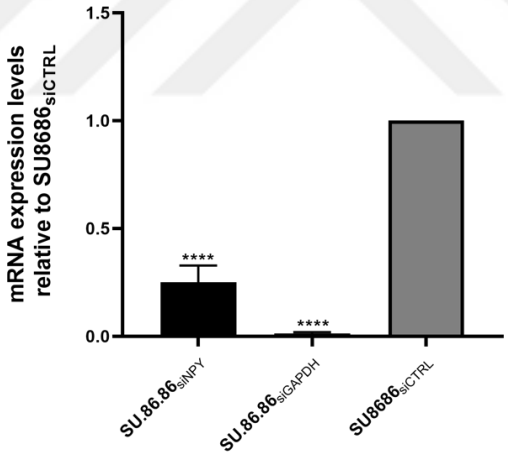

Figure11. siRNA transfections silenced GAPDH and NPY. qRT-PCR analysis showed GAPDH significantly depleted in SU.86.86 cells relative to siCTRL transfection indicating that silencing method is successful. Same procedure resulted as successful silencing in NPY-targeting siRNA transfection. Cyc-B was used as housekeeping gene. n=3, ****$P<0,0001$.

After silencing, any morphological change and decreases cell viability was not observed under the microscope. To validate this observation, cell toxicity of siRNA transfection was measured by Cell Counting Kit-8 (CCK-8) which is a colorimetric assay for the determination of the number of viable cells. Dehydrogenases in cell

reduces the substrate and produce orange colored product called formazan (35). The amount of formazan is directly proportional to the number of living cells. There was not significant difference between NPY-silenced and siCTRL transfected SU.86.86 cells (Figure 12). By this result, silencing of NPY in further functional experiments will be accepted to have no toxic effect on cells.

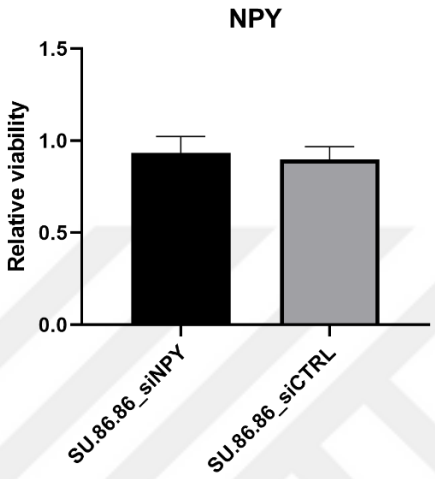

Figure 12. Cell toxicity assay for NPY depletion in SU.86.86 cells. CCK-8 kit is used to determine cell viability after siRNA transfection. It was shown that gene manipulation via application of RNAi had no effect on cell viability. n=3, ns.

4.4 In Vitro Functional Assays

In order to elucidate the cellular effects of NPY in pancreatic cancer cells, cell lines with the highest and the lowest NPY expression were subjected to *in vitro* functional assays, including proliferation, motility, migration, and invasion assays. siRNA silencing of NPY was applied to SU.86.86 cells and compared with siCTRL transfected SU.86.86 cells. T3M4 cells were treated with 10-7M human NPY in cell culture medium overnight, similar to previously applied in a different study (36). HPDE cells were used as negative control of invasive cancer cells SU.86.86 and T3M4. Those functional assays investigate cell proliferation, motility, and invasion ability of the cells. Expressional modification and complementation of NPY enable this study to describe NPY's effect on cancer cell behavior.

4.4.1 Colony formation Assay

Clonogenic assay performed to measure the capacity of seeded single cells to form into colonies. Images of colonies after the termination of the experiment at the day of 13, crystal violet staining and colony numbers are shown in Figure 13. NPY knockdown with siRNA transfection in SU.86.86 cells did not affect the colony forming capacity. hNPY pretreated T3M4 cells seems to form slightly less colonies, no significant difference detected due to the induction of NPY compared to non-treated cells.

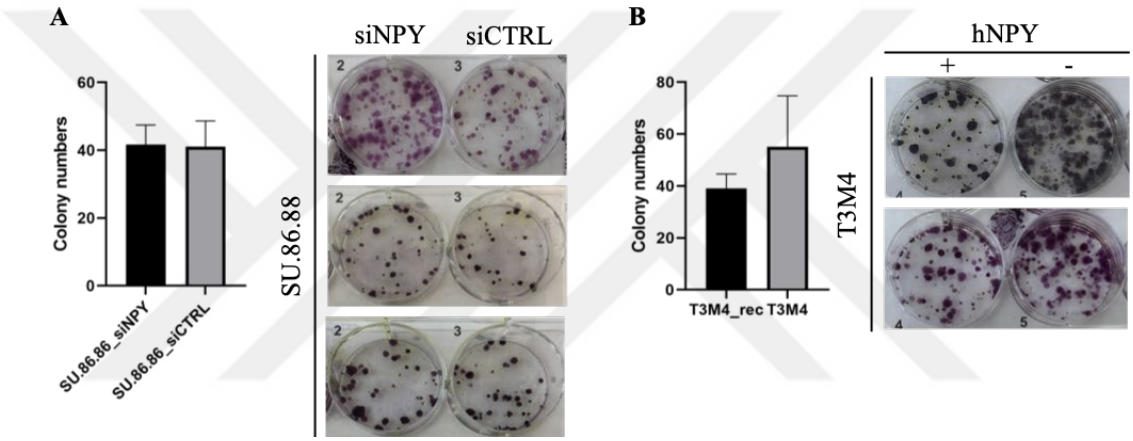

Figure 13. Colony formation assay for gene manipulation and NPY treatment. Crystal violet stained colonies after the termination of experiment. (A) NPY silencing did not influence the colony forming capacity of SU.86.86 cells. n=3, ns. (B) Overnight pretreatment of NPY did not significantly influence colony forming capacity of T3M4. n=2, ns.

4.4.2 Scratch assay

Scratch assay shows the basic migration and proliferation ability of cells by measuring the wound area, over time. To see the effect of NPY knockdown in SU.86.86 cells on wound healing capacity. SU.86.86 cells were transfected with siRNA targeting NPY and siCTRL. After overnight incubation, scratch was made on a cell monolayer and images was captured starting t=0. Percentage of covered wound area between t=0 and t=6h was calculated. (Figure 14A). Cells were collected after the live cell imaging and NPY expression was determined by qRT-PCR in order to validate whether NPY was silenced during the experiment (Figure 14B). NPY was

successfully silenced at 80%, nevertheless NPY knockdown did not affect cell migration and proliferation of SU.86.86.

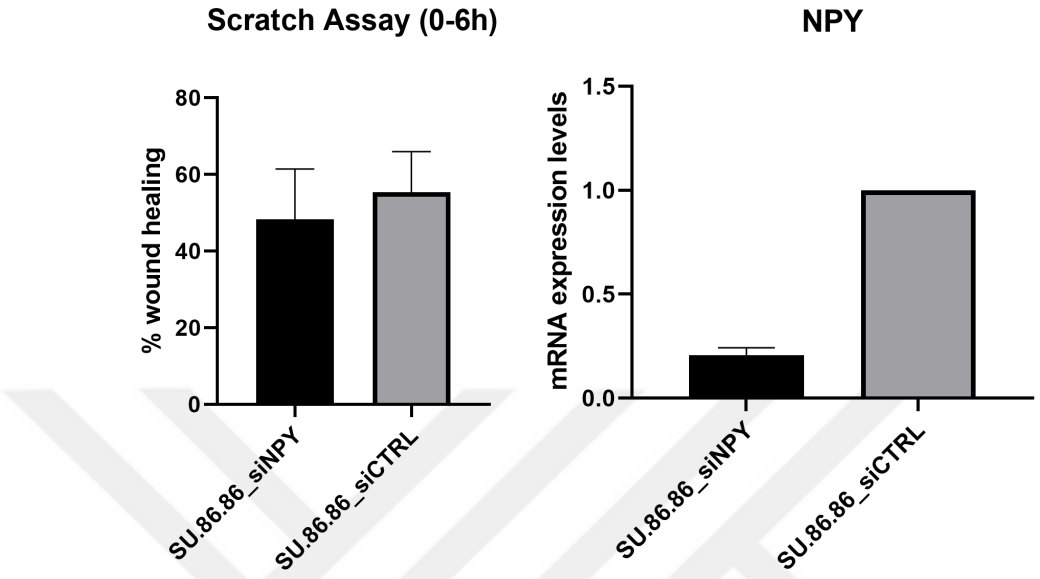

Figure 14: Scratch assay for NPY knockdown. (A) Percentage of wound healing ability of siRNA transfected SU.86.86 cells between t=0 and t=6h. Cell. Migration was not affected by NPY silencing. n=3, ns. (B) qRT-PCR validation of NPY expression of cells after scratch assay. NPY was 80% silenced in SU.86.86 cells at the end of the experiment. n=3, ****$P<0,0001$.

4.4.3 Trans-well invasion assay

Matrigel-based invasion assay provides an *in vitro* system to study cell invasion, in this study SU.86.86 and T3M4 cells were subjected under certain treatments. Invasion chambers were coated with Matrigel for assay for assessment of invasion capacity of the cells towards a chemoattractant. By this application this assay was differentiated from a migration assay. Metastatic potential and behavior of tumor cells can be studied with this method by altering interested proteins which do and might influence invasive feature of the cells like matrix degradation or cytoskeletal dynamics.

Cancer cells were seeded in the upper chamber of inserts as mono-cultures and co-cultures with hSC as a chemoattractant. In both cases, gene manipulation and complementation were applied to tumor cells. NPY was silenced with RNAi in

SU.86.86 cells (Figure 15A) and T3M4 cells were pretreated with hNPY (Figure 15B) prior to be seeded in invasion chambers which then placed in plates with and without hSC. After 3 days of incubation invaded cells, which were located at the bottom of the matrigel-coated membrane, were fixed and DAPI-stained (Figure 16A). DAPI stained cells were counted by ImageJ software. Invaded cell counts of treated and untreated were compared in two groups which are mono-cultured and co-cultured cells.

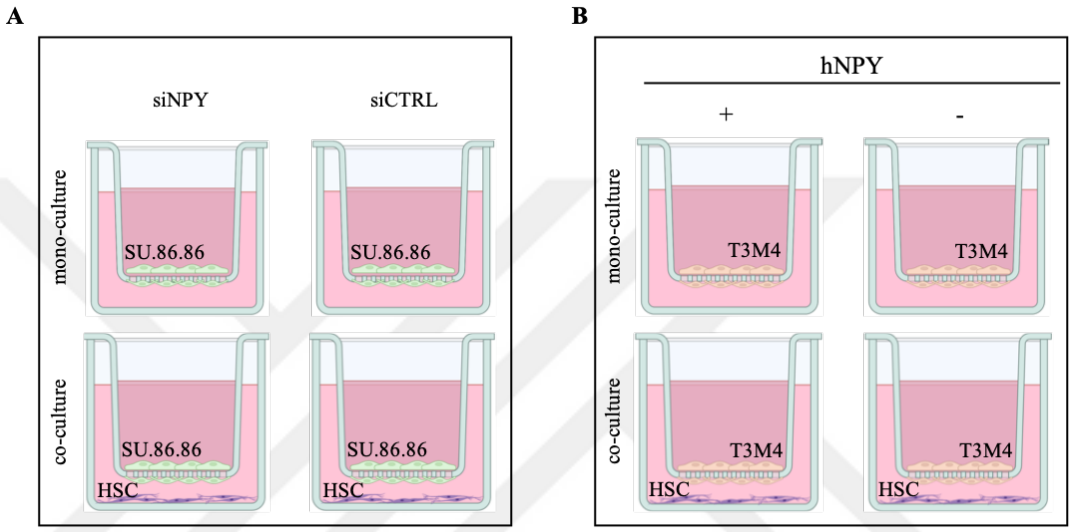

Figure 15. Matrigel-based trans-well invasion assay experimental design of (A) SU.86.86 cells and (B) T3M4 cells.

NPY silencing in SU.86.86 cells significantly decreased the number of invaded cells in the mono-cultures. siNPY transfected group showed 50% less invasiveness relative to siCTRL transfected group. When this assessment was done in the cells co-cultured with hSC, the outcome was slightly opposite. Invasion tendency seems to be increased in the case of NPY depletion in SU.86.86 cells (Figure 16B). At mRNA level, T3M4 was the line with the lowest NPY expression, when these cells pre-treated with hNPY, they showed significantly decreased invasiveness in the mono-culture. When it is compared to non-treated group, less then 50% cells were counted at the bottom of the membrane. In the co-cultures with hSC, hNPY treatment increased the tendency of cell invasion towards the lower chamber, but results were not statistically significant (Figure 16C).

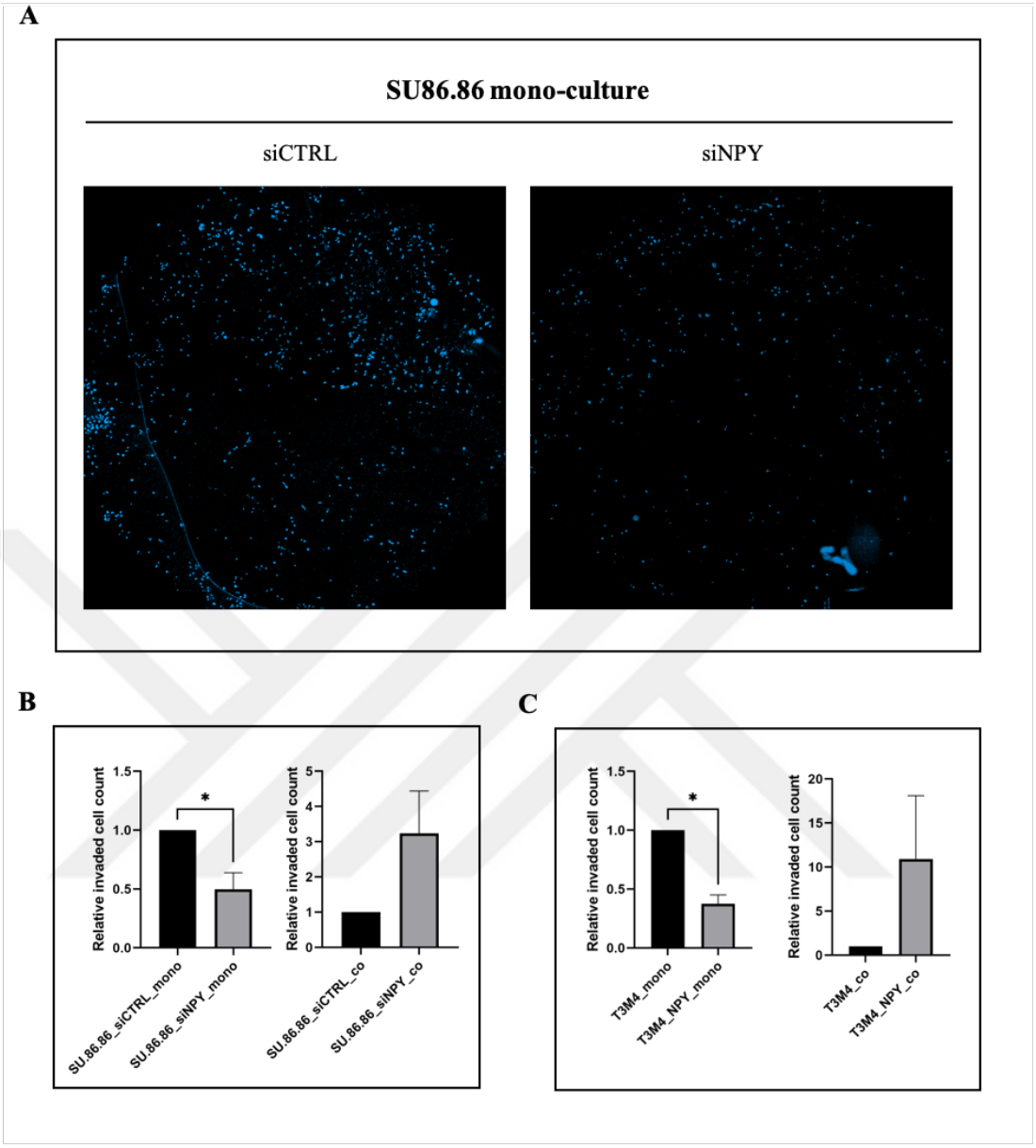

Figure 16. Matrigel-based invasion assay results. (A) DAPI-stained representative experiment of n=3 biological replicates are shown of the invaded cells at the bottom of matrigel-coated membrane. siNPY transfected SU.86.86 cells (left) and siCTRL transfected SU.86.86 cells (right) in mono-cultures. (B) Invaded cell counts of SU.86.86 cells relative to siCTRL transfected group. In mono-culture, siNPY transfected cells showed significantly less invasiveness compared to control. n=3, **P=0.0029.* In co-cultures, NPY depletion slightly increased the invasiveness of SU.86.86 towards hSC. n=3, ns. (C) Invaded cell counts of T3M4 cells relative to untrated control group. In mono-culture, hNPY treated cells showed significantly less invasiveness compared to control. n=3, **P=0.0014.* In co-cultures, hNPY treatment slightly increased the invasiveness of T3M4 towards hSC. n=3, ns.

5 DISCUSSION

Neural invasion in pancreatic cancer has become an attractive field of study due to its strong relation with tumor progression and local recurrence (18). To target NI in pancreatic cancer, a better understanding of the concept's heterotypic relations of cells and contributory mediators is necessary. Our group first characterized TPAC model of PDAC as the first GEMM that exhibits human-like NI. In this Ph.D. study, Demir showed increased expression of NPY in this model compared to the non-neuro-invasive KPC model (3). This present study was designed to investigate the role of NPY in pancreatic cancer in terms of NI.

In the first step, human pancreatic tumor samples were analyzed histologically, and NPY was found to be overexpressed in PCa compared to NP. Whereas in another study, NPY expression at mRNA level was determined by qRT-PCR and it was not increased in the tissue samples of pancreatic cancer (37). Despite the NP tissue containing more islets of Langerhans in which endocrine cells express NPY, immunoreactivity remained significantly high in human PCa tumor samples. Thus, the Quantification method was designed so that islets are excluded from the quantified area and specify the method to the exocrine pancreas. Immunohistochemical analysis strengthened this study's hypothesis. The next step is to increase the sample cohort, and the next question is to understand whether there is a relation between NPY overexpression and pain. To do that pain degree and severity of patients in the cohort will be analyzed.

NPY expression was not uniformly distributed between PCa cell lines which led the study to focus on two cell lines so that one of them has the highest and the other one has the lowest NPY expression. Both cell lines were known to be invasive, and this offers a better understanding of the cellular effects of NPY by naturally equaling the behavioral differences. NPY expression level at RNA and protein levels did not provide the same profile. This will increase the complexity of the study in the future. Y4R and Y5R were found to be expressed in nearly all PCa cell lines. CAPAN-1 expressed all receptors; on the other hand, BxPC-3 expressed none at protein level.

Nonuniform expression profiles of the receptors could be because of where cell lines originated. The differential presence of receptor types between cells may indicate different regulation and subcellular effects of NPY in PCa cells.

RNAi silencing was successful and useful method to study protein function *in vitro*. However, the method might not be very applicable for experiments requiring longer incubation time because of the limited silencing effect of siRNAs. For those purposes, gene knock-down or stable expression systems should be developed.

Functional assays provide an understanding of cellular effects of NPY in a two-sided way, in other words, by both validations of a specific effect and negative confirmation of another behavior. Such as scratch assay showed that cancer cells have higher wound healing capacity, which can be interpreted as better motility and migratory behavior as expected. At the same time, siRNA silencing of NPY did not significantly change these abilities of SU.86.86 cells, indicating that NPY does not affect cell migration in terms of wound healing. This does not mean that targeted migration is not affected by NPY, especially towards neurons. On the contrary, this strengthens the possibility that NPY specifically affects targeted invasion and does not directly affect the overall migratory behavior of cancer cells. Validation of silencing in this functional assay after the experiment was critical to show that hNPY depletion was maintained throughout the period.

Colony forming ability of cancer cells was not affected by NPY depletion in SU.86.86, and despite the slight decrease in hNPY pre-treated T3M4, no statistical difference was observed. Silencing did not change the survival and ability of NPY overexpressing cell line to grow into a colony.

Trans-well invasion assay showed that inhibition of NPY expression in SU.86.86 cells decreased the number of cells that invaded through ECM coated membrane significantly in mono-culture. On the contrary, in co-cultures, invasiveness of NPY depleted SU.86.86 cells seemed to be increased, but it was not statistically significant. This situation brings the possibility of paracrine effect of NPY or any other ligand of

NPY receptors which is secreted from hSC. NPY pre-treated T3M4 cells, similarly showed significantly decreased invasion in mono-culture. NPY overexpression plasmid will be a better approach to interpret the autocrine role of the NPY low expressing T3M4. Regarding experiments are in progress. Also, to better understand the invasive behavior of the cells, *in vitro* 3D migration assay will be performed, which is a better representative of investigating invasive behaviors of cancer cells to neurons. Initiation and very early stages of migration can be observed in real-time. Mutual tropism between cancer cells and neurons can be put under the microscope in more detail, with a broader perspective than formerly available methods.

6 CONCLUSION

This study showed that NPY is significantly overexpressed in the human pancreatic cancer tissue compared to the normal pancreas. This thesis becomes prominent and authentic by presenting immunohistochemical analysis and localization of NPY in human PCa tumor samples. *In vitro* assays gave a clue about the role of NPY in invasion while eliminating the possible subcellular functions related to proliferation and migration. Those experiments ensure the study canalizes into neural invasion. Expression profiles of NPY receptors were analyzed for the first time. One of the importance of this characterization is understanding and classifying which cell lines could be used for what purposes in future experiments. In this study, the effect of high NPY level on neural migration in invasive cancers was investigated in detail for the first time. As far as functional assays showed, although NPY has no significant effect on proliferation and motility, it seems to affect invasion. However, more decisive results will be obtained by 3D migration assay. If elevated NPY expression in pancreatic cancer, which was shown here, would be found directly proportional to the pain severity of patients, this study may be indicative of therapeutically targeting the NPY signaling pathway for neural invasion in pancreatic cancer. At the same time, this study can be seen as a starting point for investigating and finding the effector pathways and proteins involved in NPY-mediated neural invasion. Possible candidate proteins to be studied could be cytoskeleton proteins, collagenases, matrix metalloproteinases, and targeted therapies can be developed based on NPY and possible proteins directly or indirectly interacting with it.

7 REFERENCES

1. Siegel RL, Miller KD, Fuchs HE, Jemal A. Cancer statistics, 2022. CA Cancer J Clin. 2022 Jan;72(1):7-33.
2. Hishinuma S, Ogata Y, Tomikawa M, Ozawa I, Hirabayashi K, Igarashi S. Patterns of recurrence after curative resection of pancreatic cancer, based on autopsy findings. J Gastrointest Surg. 2006 Apr;10(4):511-8.
3. Demir IE. Transcriptional and functional characterization of the first neuro-invasive, genetically engineered mouse model of pancreatic cancer [Ph.D.]. Technical University of Munich, Germany; 2015.
4. Reinus J, Simon D. Gastrointestinal Anatomy and Physiology. Chichester: Wiley-Blackwell; 2014.
5. Bray F, Ferlay J, Soerjomataram I, Siegel RL, Torre LA, Jemal A. Global cancer statistics 2018: Globocan estimates of incidence and mortality worldwide for 36 cancers in 185 countries. Cancer J. Clin. 2018
6. Rawla P, Sunkara T, Gaduputi V. Epidemiology of Pancreatic Cancer: Global Trends, Etiology and Risk Factors. World Journal of Oncology. 2019;10(1):10-27.
7. Rahib L, Smith B, Aizenberg R, Rosenzweig A, Fleshman J, Matrisian L. Projecting Cancer Incidence and Deaths to 2030: The Unexpected Burden of Thyroid, Liver, and Pancreas Cancers in the United States. Cancer Research. 2014;74(11):2913-2921.
8. Chari ST, Kelly K, Hollingsworth MA, Thayer SP, Ahlquist DA, Andersen DK, Batra SK, Brentnall TA, Canto M, Cleeter DF, Firpo MA, Gambhir SS, Go VL, Hines OJ, Kenner BJ, Klimstra DS, Lerch MM, Levy MJ, Maitra A, Mulvihill SJ, Petersen GM, Rhim AD, Simeone DM, Srivastava S, Tanaka M, Vinik AI, Wong DPancreas. 2015 Jul; 44(5):693-712.
9. Mohammed S, Van Buren G 2nd, Fisher WE. Pancreatic cancer: advances in treatment. World J Gastroenterol. 2014;20(28):9354–9360.
10. Basturk O, Hong S, Wood L, Adsay N, Albores-Saavedra J, Biankin A et al. A Revised Classification System and Recommendations From the Baltimore Consensus Meeting for Neoplastic Precursor Lesions in the Pancreas. American Journal of Surgical Pathology. 2015;39(12):1730-1741.
11. Wood L, Yurgelun M, Goggins M. Genetics of Familial and Sporadic Pancreatic Cancer. Gastroenterology. 2019;156(7):2041-2055.
12. Asimgil H, Ertetik U, Çevik N, Ekizce M, Doğruöz A, Gökalp M et al. Targeting the undruggable oncogenic KRAS: the dawn of hope. JCI Insight. 2022;7(1).
13. Cornish T, Hruban R. Pancreatic Intraepithelial Neoplasia. Surgical Pathology Clinics. 2011;4(2):523-535.
14. Drapiewski J. Carcinoma of the Pancreas: A Study of Neoplastic Invasion of Nerves and its Possible Clinical Significance. American Journal of Clinical Pathology. 1944;14(11):549-556.

15. Ceyhan G, Bergmann F, Kadihasanoglu M, Altintas B, Demir I, Hinz U et al. Pancreatic Neuropathy and Neuropathic Pain—A Comprehensive Pathomorphological Study of 546 Cases. Gastroenterology. 2009;136(1):177-186.e1.
16. Liebl F, Demir IE, Mayer K, Schuster T, D'Haese JG, Becker K, Langer R, Bergmann F, Wang K, Rosenberg R, Novotny AR, Feith M, Reim D, Friess H, Ceyhan GO. The impact of neural invasion severity in gastrointestinal malignancies: A clinicopathological study. Ann Surg. 2014;**260**:900–7; discussion 907-8.
17. Schorn S, Demir IE, Haller B, Scheufele F, Reyes CM, Tieftrunk E, Sargut M, Goess R, Friess H, Ceyhan GO. The influence of neural invasion on survival and tumor recurrence in pancreatic ductal adenocarcinoma - A systematic review and meta-analysis. Surg Oncol. 2017 Mar;26(1):105-115.
18. Kayahara M, Nakagawara H, Kitagawa H, Ohta T. The Nature of Neural Invasion by Pancreatic Cancer. Pancreas. 2007;35(3):218-223.
19. Demir I, Ceyhan G, Liebl F, D'Haese J, Maak M, Friess H. Neural Invasion in Pancreatic Cancer: The Past, Present and Future. Cancers. 2010;2(3):1513-1527.
20. Makohon-Moore A, Brosnan J, Iacobuzio-Donahue C. Pancreatic cancer genomics: insights and opportunities for clinical translation. Genome Medicine. 2013;5(3):26.
21. Schwartz T, Fuhlendorff J, Kjems L, Krıstensen M, Vervelde M, O'hare M et al. Signal Epitopes in the Three-Dimensional Structure of Neuropeptide Y. Annals of the New York Academy of Sciences. 1990;611(1 Central and P):35-47.
22. Ruscica M, Dozio E, Motta M, Magni P. Relevance of the neuropeptide Y system in the biology of cancer progression. Curr Top Med Chem. 2007;7(17):1682-91.
23. Reubi JC. Peptide receptors as molecular targets for cancer diagnosis and therapy. Endocr Rev 2003;24:389–427.
24. Abualsaud N, Caprio L, Galli S, Krawczyk E, Alamri L, Zhu S et al. Neuropeptide Y/Y5 Receptor Pathway Stimulates Neuroblastoma Cell Motility Through RhoA Activation. Frontiers in Cell and Developmental Biology. 2021;8.
25. Desai D, Shende P. Strategic Aspects of NPY-Based Monoclonal Antibodies for Diagnosis and Treatment of Breast Cancer. Curr Protein Pept Sci. 2020;21(11):1097-1102.
26. Ding Y, Lee M, Gao Y, Bu P, Coarfa C, Miles B et al. Neuropeptide Y nerve paracrine regulation of prostate cancer oncogenesis and therapy resistance. The Prostate. 2020;81(1):58-71.
27. Dietrich P, Wormser L, Fritz V, Seitz T, De Maria M, Schambony A, Kremer AE, Günther C, Itzel T, Thasler WE, Teufel A, Trebicka J, Hartmann A, Neurath MF, von Hörsten S, Bosserhoff AK, Hellerbrand C. Molecular crosstalk between Y5 receptor and neuropeptide Y drives liver cancer. J Clin Invest. 2020 May 1;130(5):2509-2526.
28. Hofmann S, Maschauer S, Kuwert T, Beck-Sickinger AG, Prante O. Synthesis and in vitro and in vivo evaluation of an (18)F-labeled neuropeptide Y analogue for imaging of breast cancer by PET. Mol Pharm. 2015 Apr 6;12(4):1121-30.
29. Korner M, Reubi JC. NPY receptors in human cancer: a review of current knowledge. Peptides. 2007;28:419e425.

30. Ozaki H, Hiraoka T, Mizumoto R, Matsuno S, Matsumoto Y, Nakayama T et al. The prognostic significance of lymph node metastasis and intrapancreatic perineural invasion in pancreatic cancer after curative resection. Surgery Today. 1999;29(1):16-22.
31. De Felice E, Giaquinto D, Damiano S, Salzano A, Fabroni S, Ciarcia R et al. Distinct Pattern of NPY in Gastro–Entero–Pancreatic System of Goat Kids Fed with a New Standardized Red Orange and Lemon Extract (RLE). Animals. 2021;11(2):449.
32. Rodnoi P, Rajkumar M, Moin A, Georgia S, Butler A, Dhawan S. Neuropeptide Y expression marks partially differentiated β cells in mice and humans. JCI Insight. 2017;2(12).
33. Deer E, González-Hernández J, Coursen J, Shea J, Ngatia J, Scaife C et al. Phenotype and Genotype of Pancreatic Cancer Cell Lines. Pancreas. 2010;39(4):425-435.
34. De Oliveira T, Abiatari I, Raulefs S, Sauliunaite D, Erkan M, Kong B et al. Syndecan-2 promotes perineural invasion and cooperates with K-ras to induce an invasive pancreatic cancer cell phenotype. Molecular Cancer. 2012;11(1).
35. Ishiyama M. A highly water-soluble disulfonated tetrazolium salt as a chromogenic indicator for NADH as well as cell viability. Talanta. 1997;44(7):1299-1305.
36. Dai W, Liu Y, Zhang Y, Sun Y, Sun C, Zhang Y et al. Expression of neuropeptide Y is increased in an activated human HSC cell line. Scientific Reports. 2019;9(1).
37. Waldmann J, Fendrich V, Reichert M, Hecker A, Bartsch D, Padberg W et al. Expression of neuropeptide Y and its receptors Y1 and Y2 in pancreatic intraepithelial neoplasia and invasive pancreatic cancer in a transgenic mouse model and human samples of pancreatic cancer. Journal of Surgical Research. 2018;223:230-236.

8 CURRICULUM VITAE